A&A 429, 309–316 (2005)
DOI: 10.1051/0004-6361:20041007


Astronomy & Astrophysics

# Orbital period variation in close binaries from radial velocity data and magnetic activity cycles⋆,⋆⋆

## II. HR 1099

A. Frasca and A. F. Lanza

INAF - Osservatorio Astrofisico di Catania, via S. Sofia 78, Città Universitaria, 95123 Catania, Italy
e-mail: afrasca@ct.astro.it

Received 2 April 2004 / Accepted 1 September 2004

**Abstract.** We studied orbital period changes in the non-eclipsing close binary HR 1099, one of the most bright members of the RS CVn class of magnetically active binary systems. Intermediate-resolution optical spectroscopy and IUE archive spectra were used to build radial-velocity curves yielding epochs of superior conjunction with an accuracy of 0.01 days. The final database ranged from 1976 to 2002 and allowed us a better assessment of the amplitude of the orbital period variation and its timescale. On the basis of such results, the mechanisms proposed to explain the observed period change were briefly discussed giving further support to the possible connection between the orbital period modulation and the change of the gravitational quadrupole moment of the K1 subgiant component, in the framework of the model elaborated by Lanza et al. (1998).

**Key words.** stars: binaries: close – stars: activity – stars: binaries spectroscopic – stars: individual: HR 1099

## 1. Introduction

The spectroscopic binary system HR 1099 (V711 Tau) consists of a K1 subgiant and a G5 dwarf orbiting with a period of 2.8377 days, well detached from their respective Roche lobes. It is one of the most extensively studied members of the RS CVn class of magnetically active close binaries owing to its apparent brightness ($V \sim 5.7$) and the high level of magnetic activity that manifests itself throughout the electromagnetic spectrum (cf., e.g., Rodonò et al. 1986; Donati 1999; Strassmeier & Bartus 2000; García-Alvarez et al. 2003).

Magnetic fields are produced by the hydromagnetic dynamo action maintained in the deep fast-rotating convective envelope of the K1 IV subgiant. The G5 V component has an outer convection zone with a smaller radial extension implying that its dynamo is less efficient as indicated by its lower level of activity.

The orbital period of HR 1099 was found to be variable by Donati (1999) who pointed out that the phase of the observed superior conjunction $\phi_0$ was varying with time with respect to that calculated according to the ephemeris given by Fekel (1983). He proposed a sinusoidal fit to the observed O−C variation of $\phi_0$ from 1991 to 1996 giving a period of ≈18 yr to be confirmed by extending the time interval covered by the measurements. The relative amplitude of the orbital period variation derived on the basis of this preliminary fit was $\Delta P/P \approx 1.4 \times 10^{-4}$, i.e., among the largest values observed in RS CVn and Algol systems (Hall 1989, 1990; Lanza & Rodonò 1999). The possibility that the variation of $\phi_0$ was due to a light-time effect induced by the orbital motion of HR 1099 around an unseen third body was ruled out because the expected variation of the radial velocity of the barycenter of HR 1099 was not observed. Actually, the latest radial velocity measurements by Donati et al. (2003) confirmed the constancy of the barycenter radial velocity, but indicated that the variation of $\phi_0$ can not be fitted with a simple sinusoid, implying that the orbital period cycle is longer than 18 yr.

The only viable explanation for such orbital period variations appears to be that originally proposed by Matese & Whitmire (1983) and elaborated by Applegate (1992) and Lanza et al. (1998). It assumes that the gravitational quadrupole moment of the active components of magnetically active close binaries varies versus time due to a non-linear dynamo which perturbs stellar hydrostatic equilibrium by inducing a time-varying Lorentz force and redistributing the internal angular momentum. Specifically, an increase of the gravitational quadrupole moment produces a decrease of the orbital period, whereas a decrease of the quadrupole moment causes its increase, assuming that the orbital angular momentum stays constant during the variation. The effect is instantaneous because it is mediated directly by the gravitational field without any need for a spin-orbit coupling.

⋆ Based on IUE archive data and observations collected at Catania Astrophysical Observatory, Italy.
⋆⋆ Tables 1 and 2 are only available in electronic form at the CDS via anonymous ftp to cdsarc.u-strasbg.fr (130.79.128.5) or via http://cdsweb.u-strasbg.fr/cgi-bin/qcat?J/A+A/429/309

The Applegate's mechanism is appealing because it can provide us with a new tool to study the global energy balance of non-linear dynamos as pointed out by Lanza et al. (1998) and Lanza & Rodonò (1999). In this context, the study of the orbital period variation of HR 1099 is a very interesting topic. In the present paper, we use archive IUE observations to obtain radial velocity curves for the 1980−1992 time interval for which no radial velocity data are given in the literature. Combining these new data with the radial velocity measurements obtained from our optical spectroscopy and those of other authors, we can trace the variation of the orbital period of HR 1099 from 1976 to 2002 refining the test of Applegate's mechanism.

## 2. Observations and data reduction

Since 1994 we have secured many intermediate-resolution spectra of HR 1099 in the red-wavelength region, acquired with the REOSC échelle spectrograph at the 91-cm telescope of Catania Astrophysical Observatory (OAC) using different cross-dispersers, spectrograph cameras, and CCD detectors. Those observations were primarily aimed at monitoring the variation of the H$\alpha$ emission versus the orbital phase as well as the long-term changes of the chromospheric activity level (see, e.g., Catalano et al. 1996, 2000; Frasca et al. 1996). However, the wealth of acquired spectra, fairly well distributed versus orbital phase, allowed us to obtain good radial velocity (RV) curves in each season.

In view of our interest in orbital period variations on time-scales of decades or more, we also looked for other RV curves in the literature.

HR 1099 was firstly recognized as a double-lined spectroscopic binary by Adams et al. (1924). However, the oldest useful RV measurements we found are those of Bopp & Fekel (1976). These spectra were subsequently re-analyzed, together with additional data, by Fekel (1983) who improved the orbital solution and gave the ephemeris used in all subsequent works:

$$\mathrm{HJD_{minI}} = 2\,442\,763.952 + 2.83774 \times E. \quad (1)$$

We splitted Fekel's data set into two parts, the first ranging from 1975 to 1977 and the second from 1979 to 1981 and recomputed the orbital solution to look for conjunction phase variations in this time range.

In addition to the above data, a long series of spectra of HR 1099 was acquired by Vogt et al. (1999), but no radial velocity data were published although they provided us with an upper limit of $0\overset{\mathrm{d}}{.}043$ for the variation of the epoch of superior conjunction with respect to the ephemeris in Eq. (1) from 1982 to 1992.

### 2.1. *IUE spectra*

As we did for AR Lac in Frasca & Lanza (2000; hereinafter Paper I), we looked for HR 1099 observations in the *IUE* Final Archive and we found a large number of high-resolution spectra, mainly obtained during several monitoring campaigns dedicated to the study of HR 1099 chromospheric activity (see, e.g., Rodonò et al. 1987; Andrews et al. 1988). In the best campaigns, the satellite observations are well distributed in phase also for short observing runs, a great advantage with respect to ground-based observations which are hampered by the day-night duty cycle.

The ultraviolet spectra available in the *IUE* Final Archive were extracted by means of the new image-processing system NEWSIPS (see, e.g., Nichols & Linsky 1996; Barylak & Ponz 1998). Since we were interested in the radial velocities of the photospheric lines, we did not consider chromospheric emission lines like Mg II h & k, which seem to be affected by distortions caused by plages or other chromospherically extended structures (see, e.g., Busà et al. 1999). The long-wavelength high-resolution spectra are the most useful for an analysis of the photospheric lines, because at wavelengths longer than about 2700 Å the continuum flux of both components is recorded with a sufficiently high S/N ratio. The best method to perform radial-velocity measurements in this spectral region, in which the signal is not very high and many strong absorption lines crowd together, is by cross-correlating the observed spectra with those of radial-velocity standard stars (see, e.g., Stickland & Lloyd 1999). In order to minimize instrumental offsets, we have retrieved spectra acquired in the same instrumental configuration and as close in time as possible to those of HR 1099.

We selected spectra acquired in several observing seasons with the Long Wavelength Redundant (LWR) and the Long Wavelength Prime (LWP) cameras. The first group of data consists of spectra taken with the LWR camera in the fall of 1979 (3 spectra) and in October 1981 (10 spectra). We were forced to put together two sets of spectra obtained after 2 years to obtain a nearly complete phase coverage for these first IUE observations. As a radial-velocity standard, $\alpha$ Ari (K2 III, $V_{\mathrm{R}} = -14.3$ km s$^{-1}$ also used for the optical spectra) was chosen for the 1979 spectra, and its spectrum LWR05019, observed in 1979 July 12th with the same instrumental configuration, was used in our analysis. For the 1981 spectra, we used as RV template the spectrum LWR11700 of HD 20794 (G8 V, $V_{\mathrm{R}} = +87.3$ km s$^{-1}$) acquired by IUE during the October 1981 campaign on HR 1099. The contemporaneity of templates and target spectra led to RV measurements more accurate than possible small systematic errors in the heliocentric RV of template stars reported in the literature. As we reported in Paper I, there can be systematic differences in the wavelength scale calibrations amounting up to ~20–30 km s$^{-1}$ for spectra acquired with different cameras, but even for spectra acquired with the same camera in different epochs there can be systematic shifts of a few km s$^{-1}$. We verified the wavelength stability of IUE spectra by means of a set of 29 LWP spectra of the RV standard star $\beta$ Gem (K0 III) from February 24th to March 11th, 1994. The cross-correlation of all these spectra with respect to one of them gives RV values scattered around zero with a standard deviation $\sigma = 3.4$ km s$^{-1}$.

The second data set consisted of spectra obtained in December 1982 and in February 1983 with the LWR camera. In this case, we have used the spectrum LWR15544 of $\beta$ Gem (K0 III, $V_{\mathrm{R}} = +3.3$ km s$^{-1}$) as RV template.

Three other data sets were constructed with spectra acquired with the LWP camera in 1984, in 1985–86, and 1992, respectively. We used as RV templates the spectra LWP04039 ($\alpha$ Ari, K2 III, $V_R = -14.3$ km s$^{-1}$) for 1984 data, LWP06787 ($\kappa_1$ Cet, G5 V, $V_R = +19.9$ km s$^{-1}$) and LWP09316 ($\epsilon$ Eri, K2 V, $V_R = +15.5$ km s$^{-1}$) for 1985–86 data, and LWP24324 ($\beta$ Hyi, G2 IV, $V_R = +22.7$ km s$^{-1}$) for the 1992 data set. All these stars were observed by IUE during, or very close in time to, the respective HR 1099 campaigns.

We cross-correlated each order of the HR 1099 spectra with the corresponding one of the radial velocity standard, starting from the 83rd order ($\lambda_c$ = 2750 Å) and ending at the 72nd order ($\lambda_c$ = 3170 Å) because thereafter the portion of each order covered by the detector became very small. Although the cross-correlation function (CCF) of spectra far from the conjunctions had a double-peaked appearance, the peak relative to the G5 V star (which dominates at these wavelengths) was always higher. Consequently, the radial velocity of the hotter component was much better determined, and the results from the different orders were consistent with each other. The RV measurements of the cooler component were always much worse than those of the G5 component, with errors of the order of ±(15–20) km s$^{-1}$. Hence we decided to disregard its radial-velocity curves obtained from IUE spectra in our analysis (cf. Fig. 1).

In Table 1, the IUE spectra are listed together with the heliocentric Julian date (HJD), the radial velocity of the G5 V component of HR 1099 and its error. The radial velocities are averages of the values resulting from the different orders, discarding measures outside the 3$\sigma$ range. The errors in the radial velocities were evaluated by computing the standard deviation of the measurements and were typically of a few km s$^{-1}$.

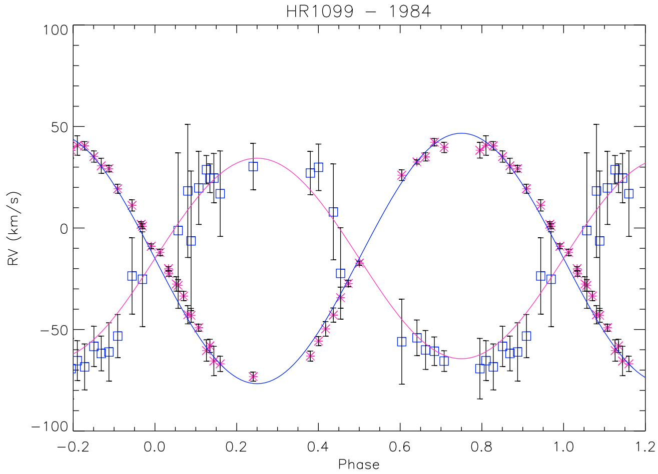


**Fig. 1.** Radial-velocity curve of HR 1099 in 1984 from IUE data. The solid lines are the radial-velocity curves computed according to the Fekel (1983) orbital solution and ephemeris. Asterisks denote the RVs of the hotter G5 V component, whereas the much more scattered RVs of the cooler K1 IV component are plotted as open squares.

### 2.2. Optical spectroscopy

The first Catania data set was obtained in the fall of 1994 and only two échelle orders were recorded, centered at about 6420 and 6600 Å. The resolving power $R \simeq 14\,000$, corresponding to a two-pixel sampling, was deduced from the full width at half maximum (FWHM) of the emission lines of the Th-Ar calibration lamp.

In 1996 and 1997 we observed HR 1099 with a new objective camera and CCD detector that were capable of recording four orders in each frame, spanning from about 6050 to 6650 Å, and nearly completely covering each échelle order.

The last two data sets were obtained in 2000 and 2001 with a new CCD detector allowing us to record five orders in each frame, spanning from about 5860 to 6700 Å.

All these spectra were acquired with a signal-to-noise ratio typically between 90 and 150, with only a few exceptions in cases of bad weather, and a resolution $R \simeq 14\,000$.

A standard data reduction was performed in all cases by means of the ECHELLE task of the package IRAF[1] (see, e.g., Frasca et al. 2000).

[1] IRAF (Image Reduction and Analysis Facilities) is distributed by the National Optical Astronomy Observatories, which are operated by the Association of Universities for Research in Astronomy, Inc., under cooperative agreement with the National Science Foundation.

Radial velocity measurements were computed by means of the cross-correlation technique using the IRAF task FXCOR (e.g., Tonry & Davis 1979; Fitzpatric 1993; Popper & Jeong 1994). The bright, slowly-rotating, radial-velocity standard stars $\alpha$ Ari ($V_R = -14.3$ km s$^{-1}$), $\alpha$ Tau ($V_R = +54.3$ km s$^{-1}$), 12 Tau ($V_R = +22.5$ km s$^{-1}$), and 31 Aql ($V_R = -100.5$ km s$^{-1}$), whose spectra were acquired during the HR 1099 observing seasons, were used as templates for the cross-correlation. We excluded from the analysis the H$\alpha$ and Na I $D_2$ lines which can be contaminated by chromospheric emission and all the spectral ranges heavily affected by telluric absorption lines (e.g., the $O_2$ band $\lambda$6276–6315).

To better evaluate the centroids of the CCF peaks (i.e. the radial velocity of the primary and secondary component) we adopted two separate Gaussian fits for the cases with a significant peak separation (i.e. far from the conjunctions), and a two-Gaussian fit algorithm to resolve cross-correlation peaks in the blended situations. In these cases, whenever we obtained a sequence of at least two consecutive spectra, we used the method introduced by Donati et al. (1992) which allows us to remove the contribution of the secondary component from the CCF and to improve the radial velocity measurements.

The radial velocities of the two components of HR 1099, listed in Table 2 together with their standard errors, are the weighted averages of the values obtained from the cross-correlation of each order of the target spectra with the corresponding order of the standard spectrum observed in the same night. The usual weight $W_i = \sigma_i^{-2}$ has been given to each measurement. The standard errors of the weighted means have been computed on the basis of the errors $\sigma_i$ in the $RV$ values for each order according to the usual formula (see, e.g., Topping 1972). The $\sigma_i$ values are computed by FXCOR according to the fitted peak height and the antisymmetric noise as described by Tonry & Davis (1979).

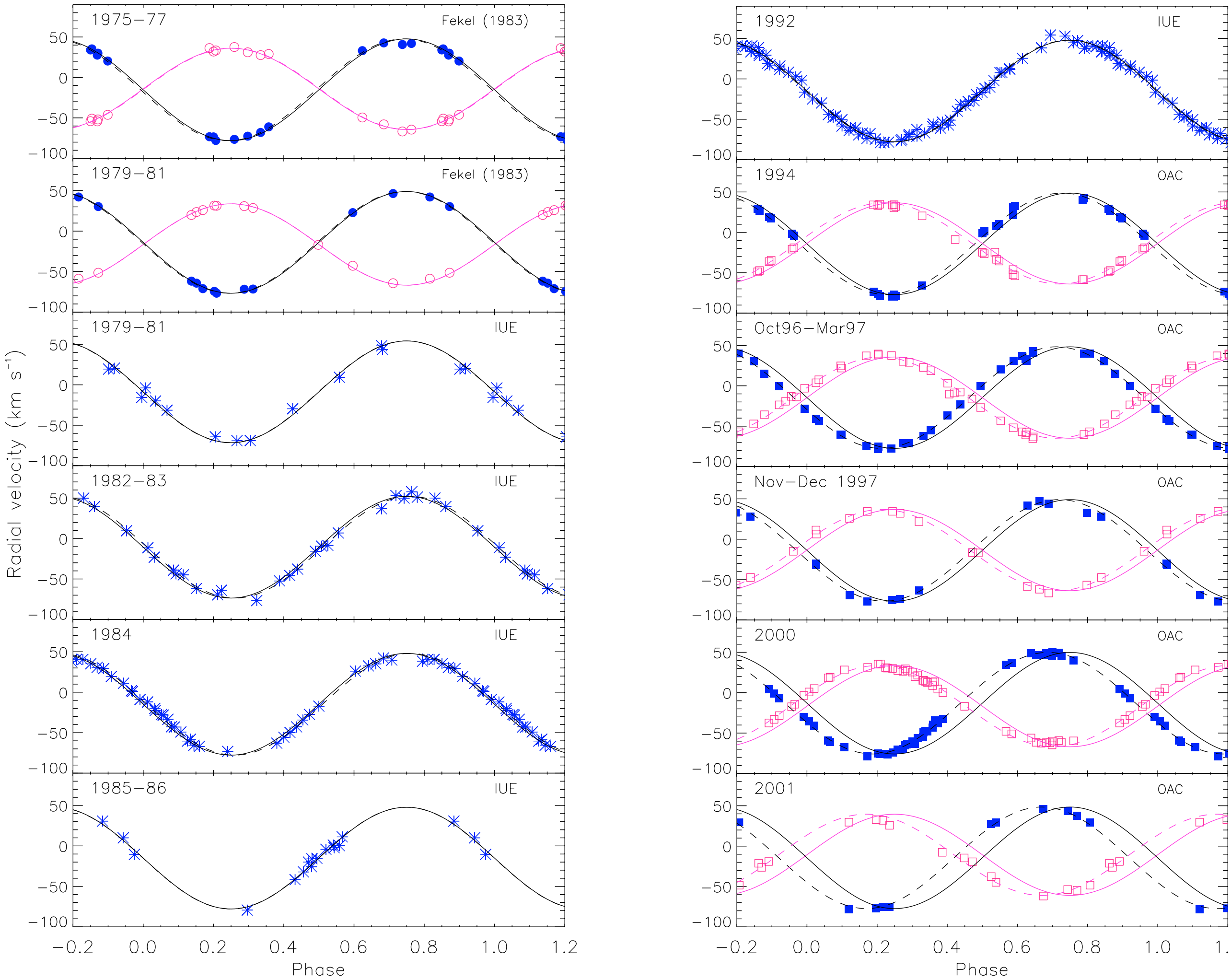


**Fig. 2.** Radial-velocity curves (circles for Fekel (1983) data, asterisks for IUE, squares for our own data) and best-fit solution of HR 1099. The solid lines are the radial-velocity curves computed according to Fekel's ephemeris (Eq. (1)), the dashed lines are the actual radial-velocity curves, fitted to the observational data by varying the phase of superior conjunction $\phi_0$.

## 3. Analysis and results

In order to check the overall goodness of our data sets and, in particular that of the radial velocities of the G5 V component derived from IUE spectra, we performed sinusoidal fits to the radial-velocity curves relative to the five IUE radial-velocity data sets. We used the CURFIT routine (Bevington 1969) based on a gradient-expansion algorithm which gives also standard deviations for the parameters. The values of the barycentric velocity $\gamma$ and RV semi-amplitudes of the hotter ($K_{\rm G5}$) and cooler ($K_{\rm K1}$, only from optical data) components determined in such a way (see Table 3) are in good agreement with those listed in García-Alvarez et al. (2003), with the exception of the data sets with poor phase coverage, or in which there were very few data near the quadratures.

After checking for the consistency of the various radial velocity-curves, we determined the differences between the epochs of superior conjunction and a fixed ephemeris. All the radial-velocity data were folded in phase with the Fekel (1983) ephemeris (Eq. (1)) and then each radial-velocity curve was fitted with a sinusoid in which $K_{\rm K1}$ and $K_{\rm G5}$ were fixed to the values $K_{K1}$ = 50.3 km s$^{-1}$ and $K_{\rm G5}$ = 62.9 km s$^{-1}$, varying the barycentric velocity $\gamma$ and the phase of superior conjunction $\phi_0$. For the data sets containing radial velocities of both components, the analysis was performed separately for both radial-velocity curves, and an average phase shift was derived. For the IUE data, only the G5 V component was taken into account.

In Fig. 2 the observed radial velocity curves are plotted, together with the radial velocity curves computed according to the Fekel ephemeris Eq. (1), and the best fit radial velocity curves obtained as explained above. The comparison clearly shows the amount of phase shift $\phi_0$.

In Table 4 we list the mean epochs of the RV data sets, the corresponding O−C, and the data reference. In the same Table we list also the O−C from the literature. The O−C's derived in the present work are plotted in Fig. 3a versus time, together with the O−C's from the literature. The availability of the present new data for the period before 1990 lead to a significant improvement of the knowledge of the O−C variations versus time. The O−C's stayed approximately constant from about 1976 to 1990 and then began to decrease steeply.

**Table 3.** Orbital elements of HR 1099 determined in the present study, with barycentric velocity ($\gamma$), semi-amplitudes ($K_{\rm K1}$, $K_{\rm G5}$) and initial phase ($\phi_0$) assumed as free parameters for the best fit.

| Mean JD | $K_{\rm K1}$ (km s$^{-1}$) | $K_{\rm G5}$ (km s$^{-1}$) | $\gamma$ (km s$^{-1}$) | Reference |
|---|---|---|---|---|
| 2 442 793 | 50.49 ± 1.49 | 61.50 ± 1.53 | −14.70 ± 0.85 | Fekel (1975–77) |
| 2 444 477 | 48.47 ± 2.60 | 62.39 ± 2.59 | −15.12 ± 1.34 | Fekel (1979–81) |
| 2 444 722 | — | 62.39 ± 2.59 | −10.38 ± 1.23 | IUE 1979–81 |
| 2 445 344 | — | 62.48 ± 0.58 | −11.65 ± 0.39 | IUE 1982–83 |
| 2 446 048 | — | 60.95 ± 0.64 | −13.73 ± 0.34 | IUE 1984 |
| 2 446 582 | — | 56.68 ± 1.99 | −15.18 ± 1.17 | IUE 1985–86 |
| 2 448 971 | — | 61.67 ± 0.25 | −15.33 ± 0.16 | IUE 1992 |
| 2 449 627 | 46.72 ± 0.96 | 63.80 ± 1.96 | −14.60 ± 0.65 | OAC 1994 |
| 2 450 421 | 51.73 ± 0.41 | 62.91 ± 1.08 | −14.75 ± 0.46 | OAC 1996 |
| 2 450 795 | 50.28 ± 0.58 | 61.77 ± 1.26 | −13.39 ± 0.54 | OAC 1997 |
| 2 451 820 | 48.13 ± 0.39 | 62.02 ± 0.86 | −15.73 ± 0.44 | OAC 2000 |
| 2 452 239 | 44.62 ± 0.67 | 64.47 ± 1.59 | −12.28 ± 0.57 | OAC 2001 |

The only point rather away from the overall O−C trend is the value derived from the IUE RV curve in 1985–86. Indeed, this curve (see Fig. 2) consists of a few data with a poor phase coverage that could have introduced a larger systematic error in the determination of $\phi_0$. Unfortunately, we did not found additional RV data in the literature to verify whether such relatively wide O−C variation really occurred or not.

## 4. Discussion

We fitted the O−C variations by a low-order polynomial, excluding the O−C value of 1985. The $\chi^2$ of the fit is rather high for a parabola ($\chi^2$ = 28.6) and decreases significantly for polynomials of degree $n$ = 3 ($\chi^2$ = 12.6) and $n$ = 4 ($\chi^2$ = 7.9), remaining essentially the same for $n$ = 5 and then marginally decreasing for $n$ = 6 ($\chi^2$ = 6.0). Therefore, we adopted the 4th degree polynomial as the best representation of the O−C variations, minimizing the number of the degrees of freedom of the fit.

The residuals of the O−C's with respect to the fitting polynomial are shown in Fig. 3b. They are larger than the accuracy of the individual measurements likely due to the distortion of the line profiles induced by the cool starspots on the photospheres of the components (see, e.g., Paper I). The amplitude of the dispersion is $\sim 0^{\rm d}\!.015$ as shown by comparing nearly simultaneous measurements by different observatories. Nevertheless, we made a periodogram analysis of the residuals (Scargle 1982; Horne & Baliunas 1986) finding some concentration of power around a period of about 8 years, with a false alarm probability of ≈60%, that is not significant.

The possibility that the O−C variation is due to a light-time effect was already excluded by Donati (1999) and the present data reinforce his conclusion.

Apart from a zero scale offset, the velocity of the center of mass of the binary system can be obtained from the derivative of the O−C variation versus time (Irwin 1952). We calculated it using the fitting polynomial and compared it with the measured

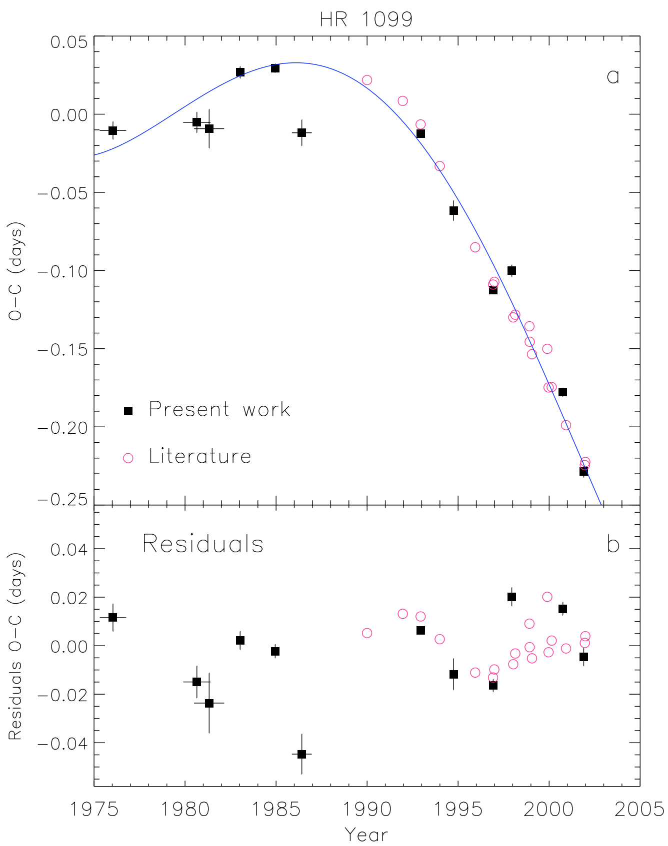


**Fig. 3. a)** O−C orbital variations of HR 1099 vs. time. The O−C were computed with respect to the ephemeris reported in Eq. (1). The O−C's determined in the present paper are displayed as filled squares, while those from the literature are plotted as open circles. The vertical error-bars denote the standard deviation of our O−C as derived from the CURFIT routine, whereas the horizontal bars indicate the range of the epochs of the corresponding RV curve. For the literature data the errors are comparable with the symbol size. The solid line is the 4th order polynomial best fit to the O−C variations (see the text). **b)** The residuals of the O−C variation with respect to the 4th order polynomial fit. Symbols are the same as in the upper panel.

**Table 4.** O−C's from spectroscopic orbits.

| Mean JD | Mean epoch | O−C (days) | $\gamma^a$ (km s$^{-1}$) | Reference |
|---|---|---|---|---|
| 2 442 793 | 1976.04 | −0.010 ± 0.006 | −14.7 | Fekel (1975–77)[b] |
| 2 444 477 | 1980.65 | −0.005 ± 0.007 | −15.3 | Fekel (1979–81)[b] |
| 2 444 722 | 1981.32 | −0.009 ± 0.012 | −10.4 | IUE 1979–81 |
| 2 445 344 | 1983.02 | 0.027 ± 0.004 | −11.6 | IUE 1982–83 |
| 2 446 048 | 1984.95 | 0.029 ± 0.003 | −14.0 | IUE 1984 |
| 2 446 582 | 1986.42 | −0.012 ± 0.008 | −16.4 | IUE 1985–86 |
| 2 448 971 | 1992.95 | −0.012 ± 0.002 | −15.2 | IUE 1992 |
| 2 449 627 | 1994.75 | −0.062 ± 0.006 | −13.7 | OAC 1994 |
| 2 450 421 | 1996.92 | −0.112 ± 0.002 | −14.6 | OAC 1996 |
| 2 450 795 | 1997.95 | −0.100 ± 0.004 | −13.8 | OAC 1997 |
| 2 451 820 | 2000.76 | −0.178 ± 0.003 | −15.7 | OAC 2000 |
| 2 452 239 | 2001.90 | −0.229 ± 0.004 | −14.4 | OAC 2001 |
| 2 447 892 | 1990.00 | 0.0219 ± 0.0011 | −15.4 | Donati (1999) |
| 2 448 607 | 1991.96 | 0.0085 ± 0.0011 | −14.9 | " " |
| 2 448 965 | 1992.94 | −0.0065 ± 0.0011 | −15.0 | " " |
| 2 449 349 | 1993.99 | −0.0332 ± 0.0011 | −15.0 | " " |
| 2 450 060 | 1995.94 | −0.0851 ± 0.0011 | −14.9 | " " |
| 2 450 445 | 1996.99 | −0.1073 ± 0.0011 | −14.3 | " " |
| 2 450 419 | 1996.92 | −0.1090 ± 0.0011 | −15.9 | Strassmeier & Bartus (2000) |
| 2451149 | 1998.92 | −0.1356 ± 0.0011 | −15.6 | García-Alvarez et al. (2003) |
| 2 450 825 | 1998.03 | −0.1300 ± 0.0003 | −14.5 | Donati et al. (2003) |
| 2 450 864 | 1998.14 | −0.1283 ± 0.0006 | −14.2 | Petit et al. (2004) |
| 2 451 155 | 1998.93 | −0.1456 ± 0.0006 | −13.8 | Petit et al. (2004) |
| 2 451 201 | 1999.06 | −0.1535 ± 0.0006 | −14.5 | Petit et al. (2004) |
| 2 451 507 | 1999.90 | −0.1501 ± 0.0003 | −14.6 | Donati et al. (2003) |
| 2 451 532 | 1999.97 | −0.1748 ± 0.0003 | −14.7 | " " |
| 2 451 595 | 2000.14 | −0.1745 ± 0.0006 | −14.2 | Petit et al. (2004) |
| 2 451 884 | 2000.93 | −0.1989 ± 0.0003 | −14.8 | Donati et al. (2003) |
| 2 452 263 | 2001.96 | −0.2245 ± 0.0006 | −14.6 | Petit et al. (2004) |
| 2 452 271 | 2001.99 | −0.2225 ± 0.0003 | −14.5 | Donati et al. (2003) |

[a] The barycentric velocity $\gamma$ for IUE and OAC data was determined by fixing $K_{K1}$ and $K_{G5}$ in the best-fit procedure.
[b] Original data from Fekel (1983) re-analyzed in the present paper.

$\gamma$ values in Fig. 4. The expected $\gamma$ variation from 1980 to 2000 was larger than 25 km s$^{-1}$, whereas the measured barycentric velocity stayed nearly constant within a few km s$^{-1}$.

The rate of the orbital period variation can be calculated by means of the polynomial fit (e.g., Kalimeris et al. 1994) and is shown in Fig. 5. The relative variation amounts to $\Delta P/P \simeq 9.0 \times 10^{-5}$ from 1980 to 2000, i.e., ≈60% of that estimated by Donati (1999) who could rely only on data from 1990.

Various physical mechanisms involving mass loss in a magnetized stellar wind or the magnetic interaction between the components were considered by Donati (1999) in order to explain such a large variation on a so short time scale. They were rejected because the required mass loss rate or coronal magnetic field intensities were implausibly large, i.e., at least 2−3 orders of magnitude larger than allowed by the observations.

The only mechanism that does not appear seriously at variance with the observational constraints is that proposed by Lanza et al. (1998) as an extension of the model originally due to Applegate (1992). The relative angular velocity variation of the outer layers of the K1 IV component required by the model of Lanza et al. (1998) with $\Delta P/P = 9.0 \times 10^{-5}$, adopting the stellar parameters given by Donati (1999), is: $\Delta\Omega/\Omega \simeq 1.7 \times 10^{-2}$. Such a value is indeed about 3 times the amplitude of the surface differential rotation as derived by using starspots as tracers (Petit et al. 2004, and references therein) and it compares quite well with the typical variations required to explain the observed orbital period changes in Algol's and RS CVn binaries (cf. Lanza & Rodonò 1999). It is important to note that the low inclination of the rotation axis of the K1 IV component ($i \sim 38°$) and the active longitudes of the starspot activity may affect the determination of the surface differential rotation

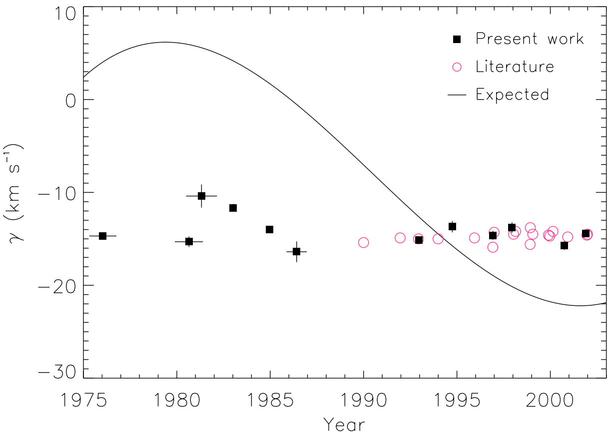


**Fig. 4.** Barycentric velocity of HR 1099 vs. time. The values of $\gamma$ determined in the present paper are displayed as filled squares, while those from the literature are represented by open circles. The vertical error-bars denote the standard deviation of our measurements as derived from the CURFIT routine, whereas the horizontal bars indicate the range of the epochs of the corresponding RV curve. For the literature data the errors are comparable with the symbol size. The scatter is higher for the IUE data that may be affected by systematic errors.

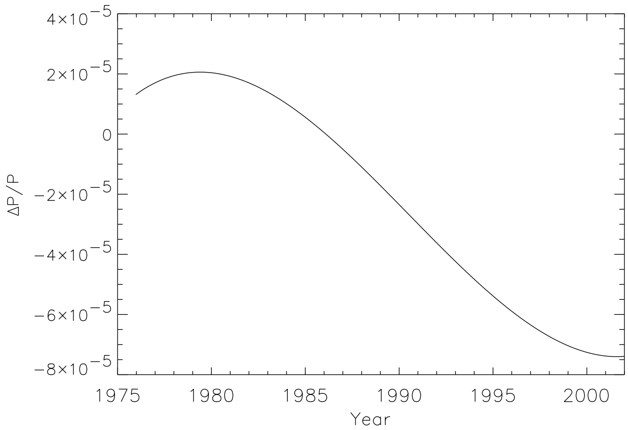


**Fig. 5.** Orbital period variation ($\Delta P/P$) of HR 1099 versus time as derived by the 4th order polynomial best fit to the O−C variations.

based on the drift of photospheric spots (Henry et al. 1995; Eaton et al. 1996). Therefore, the reported amplitudes should be regarded as lower limits, thus improving the agreement between model prediction and observations.

The detection of a variation of the surface rotation profile of the K1 IV component star versus time would represent a stringent test of Applegate's mechanism. The short lifetime of the surface features (~a few months) makes it a challenging task, but it should be possible to obtain at least an upper limit to be compared with the present estimate in the next few years (cf. Petit et al. 2004).

It is worth considering the possible connection between period change and magnetic activity cycle as revealed by long-term optical photometry. The cycle period is ≈16 yr (Henry et al. 1995; Strassmeier & Bartus 2000) that would imply an orbital period modulation cycle of ≈35 yr, according to the torsional oscillation model proposed by Lanza et al. (1998). The association between the maximum of the O−C around 1985–1990 and a maximum of the activity cycle around 1986 is also in agreement with such a model even if further observations are needed to confirm the proposed connection (cf. Lanza & Rodonò 2004).

## 5. Conclusion

The new epochs of conjunctions determined in the present work allowed us a better assessment of the timescale and amplitude of the orbital period change of the active close binary HR 1099. They gave further support to the conclusion that Applegate's mechanism in the formulation by Lanza et al. (1998) provides the least unlikely explanation for the observed period variations. However, further observations are required in order to determine the amplitude and the length of the orbital period cycle and to test the prediction on the amplitude of the variation of surface rotation rate. In fact, HR 1099 is one of the RS CVn binaries with the largest orbital period change and can provide us with a stringent test for the Applegate's mechanism.

*Acknowledgements.* The authors are grateful to an anonymous Referee and to J.-F. Donati for a careful reading of the paper and valuable comments.
This research has made use of the ADS-CDS databases, operated at the CDS, Strasbourg, France.
Active star research at INAF-Catania Astrophysical Observatory and the Department of Physics and Astronomy of Catania University is funded by MIUR (*Ministero della Istruzione, Università e Ricerca*), and the *Regione Siciliana*, whose financial support is gratefully acknowledged.

## References

Adams, W. S., Joy, A. H., & Sanford, R. F. 1924, PASP, 36, 137
Andrews, A. D., Rodonò, M., Linsky, J. L., et al. 1988, A&A, 204, 177
Applegate, J. H. 1992, ApJ, 385, 621
Barylak, M., & Ponz, J. D. 1998, in Astronomical Data Analysis Software and Systems VI, ed. R. Albrecht, R. N. Hook, & H. A. Bushouse, ASP Conf. Ser., 145, 404
Bevington, P. R. 1969, Data Reduction and Error Analysis for the Physical Sciences (McGraw-Hill Book Company), 237
Bopp, B. W., & Fekel, F. C. 1976, AJ, 81, 771
Busà, I., Pagano, I., Rodonò, M., Neff, J. E., & Lanzafame, A. C. 1999, A&A, 350, 571
Catalano, S., Rodonò, M., Frasca, A., & Cutispoto, G. 1996, in Stellar Surface Structures, ed. K. G. Strassmeier, & J. L. Linsky (Dordrecht: Kluwer Ac. Publ.), IAU Symp., 176, 403
Catalano, S., Rodonò, M., Cutispoto, G., et al. 2000, in Variable Stars as Essential Astrophysical Tools, ed. C. Ibanoglu, NATO Science Series C: Math. Phys. Sci., 544, 687
Donati, J.-F., Brown, S. F., Semel, M., et al. 1992, A&A, 265, 682
Donati, J.-F. 1999, MNRAS, 302, 457
Donati, J.-F., Cameron, A. C., Semel, M., et al. 2003, MNRAS, 345, 1145
Eaton, J. A., Henry, G. W., & Fekel, F. C. 1996, ApJ, 462, 888
Fekel, F. C. 1983, ApJ, 268, 274
Fitzpatrick, M. J. 1993, in Astronomical Data Analysis Software and System II, ed. R. J. Hanish, R. V. J. Brissenden, & J. Barnes, ASP Conf. Ser., 52, 472
Frasca, A., & Lanza, A. F. 2000, A&A, 356, 267 (Paper I)

Frasca, A., Catalano, S., & Marilli, E. 1996, in 153rd IAU Coll., Magnetodynamic phenomena in the solar atmosphere. Prototypes of stellar magnetic activity, ed. Y. Uchida, T. Kosugi, & H. S. Hudson (Dordrecht: Kluwer Academic Publishers), 475
Frasca, A., Marino, G., Catalano, S., & Marilli, E. 2000, A&A, 358, 1007
García-Alvarez, D., Foing, B. H., Montes, D., et al. 2003, A&A, 397, 285
Hall, D. S. 1989, Space Sci. Rev., 50, 219
Hall, D. S. 1990, in NATO Advanced Study Institute on Active Close Binaries, ed. C. İbanoğlu (Dordrecht: Kluwer Ac. Publ.), 95
Henry, G. W., Eaton, J. A., Hamer, J., & Hall, D. S. 1995, ApJS, 97, 513
Horne, J. H., & Baliunas, S. L. 1986, ApJ, 302, 757
Irwin, J. B. 1952, ApJ, 116, 211
Kalimeris, A., Rovithis-Livaniou, H., & Rovithis, P. 1994, A&A, 282, 775
Lanza, A. F., & Rodonò, M. 1999, A&A, 349, 887
Lanza, A. F., Rodonò, M., & Rosner, R. 1998, MNRAS, 296, 893
Lanza, A. F., & Rodonò, M. 2004, AN, 325, 393
Matese, J. J., & Whitmire, D. P. 1983, A&A, 117, L7
Nichols, J. S., & Linsky, J. L. 1996, AJ, 111, 517
Petit, P., Donati, J.-F., Wade, G. A., et al. 2004, MNRAS, 348, 1175
Popper, D. M., & Jeong, Y. C. 1994, PASP, 106, 184
Rodonò, M., Cutispoto, G., Pazzani, V., et al. 1986, A&A, 165, 135
Rodonò, M., Byrne, P. B., Neff, J. E., et al. 1987, A&A, 176, 267
Scargle, J. D. 1982, ApJ, 263, 835
Stickland, D. F., & Lloyd, C. 1999, The Observatory, 119, 16
Strassmeier, K. G., & Bartus, J. 2000, A&A, 354, 537
Tonry, J., & Davis, M. 1979, AJ, 84, 1511
Topping, J. 1972, Errors of Observation and Their Treatment (Chapman and Hall Ltd.), 89
Vogt, S. S., Hatzes, A. P., Misch, A., & Kürster, M. 1999, ApJS, 121, 547